Physics and Imaging in Radiation Oncology 25 (2023) 100415

Contents lists available at ScienceDirect

Physics and Imaging in Radiation Oncology

journal homepage: www.sciencedirect.com/journal/physics-and-imaging-in-radiation-oncology

Technical Note

Assessment of intra-fraction motion during frameless image guided Gamma Knife stereotactic radiosurgery☆

Winnie Li [a,b,*], Gregory Bootsma [a], David Shultz [a,b], Normand Laperriere [a,b], Barbara-Ann Millar [a,b], Young Bin Cho [a,b], David A. Jaffray [a,b], Caroline Chung [a,b], Catherine Coolens [a,b]

[a] Radiation Medicine Program, Princess Margaret Cancer Centre, Toronto, ON, Canada
[b] Department of Radiation Oncology, University of Toronto, Toronto, ON, Canada

ARTICLE INFO

Keywords:
Intrafraction motion
Gamma Knife
Stereotactic radiosurgery
Image guidance

ABSTRACT

As frameless stereotactic radiosurgery increase in use, the aim of this study was to evaluate intra-fraction motion through cone-beam CT (CBCT) and high-definition motion management (HDMM) systems. Intra-fraction motion measured between localization, repeat localization and post-treatment CBCTs were correlated to intra-faction motion indicated by the HDMM files using the Pearson coefficient (r). A total of 302 plans were reviewed from 263 patients (114 male, 149 female); 216 pairs of localization-repeat localization, and 260 localization–-post-treatment CBCTs were analyzed against HDMM logs. We found the magnitude of intra-fraction motion detected by the HDMM system were larger than the corresponding CBCT results.

1. Introduction

Radiation treatment for brain metastases is shifting to minimize treatment-related complications and maximize functional preservation as patient survival increases [1,2]. Rising concerns of neurocognitive toxicity following whole brain radiation has led to growing use of radiosurgery (SRS) [3]. Use of fractionated SRS has motivated the development of frameless immobilization systems [4–6]. An immobilization system consisting of a thermoplastic mask with infrared (IR) tracking through the high-definition motion management (HDMM) system in addition to CBCT image-guidance is available for Cobalt-60 SRS.

For frameless SRS, HDMM measurements through the nose tip [7] has been shown to exhibit larger intra-fraction motion when compared to CBCT [8]. A larger magnitude of intra-fraction motion was measured for patients treated in the mask when compared to frame fixation [9], and the number of treatment interruptions increased with treatment time [9–12]. As frameless SRS increase in use, it is pertinent to explore factors that may affect patient motion during treatment to inform the appropriateness of HDMM thresholds and planning target volume (PTV) margins.

The objective of this study was to quantify intra-fraction motion in the mask as detected by the HDMM system and measured on CBCTs.

2. Materials and methods

2.1. Patients

This prospective study included patients with intracranial tumors planned for frameless single-fraction or 3-fraction Gamma Knife (GK, ICON®, Elekta, Stockholm, Sweden) SRS from November 2019 – March 2021. Informed consent was obtained per Research Ethics Board guidelines.

A total of 263 patients were included in this study with 302 unique plans. The median age was 65 years, and 56 % of the patients were female. Patient characteristics are described in Table S1.

2.2. Treatment planning

Patient-specific frameless immobilization was fabricated on the GK, consisting of a custom headrest and thermoplastic mask with a nose cutout. A simulation reference 6.3 mGy CBCT was acquired after immobilization fitting with the patient in the intended treatment position. Volumetric magnetic resonance images were also acquired for

☆ This work was presented in part at the Annual Meeting of American Society for Therapeutic Radiology and Oncology, October 2020, Virtual Meeting.

* Corresponding author at: Radiation Medicine Program, Princess Margaret Cancer Centre, 610 University Avenue, Level 2B, Cobalt Lounge, Toronto, ON, Canada.
E-mail address: winnie.li@rmp.uhn.ca (W. Li).

https://doi.org/10.1016/j.phro.2023.100415
Received 26 July 2022; Received in revised form 16 January 2023; Accepted 18 January 2023
Available online 21 January 2023

treatment planning purposes, including gadolinium-enhanced axial T1 images with 1 mm slice thickness, T2 fluid attenuated inversion recovery (FLAIR) images for target (i.e. gross target volume, GTV) delineation, and CT simulation (1 mm slice thickness) for dosimetry calculations.

For single and multi-fraction SRS to solid tumors, a 1 mm PTV margin was added to the GTV. For fractionated SRS to cavity targets, a 1 mm clinical target volume (CTV) margin was added to the GTV, and a 1 mm PTV added to the CTV. All patients were planned with the GK treatment planning system (Leksell Gamma Plan version 11.1, Elekta Stockholm, Sweden). The fractionation schedules used at our institution range from 15 to 21 Gy delivered in a single fraction or 21–27 Gy delivered over 3 fractions (based on target volume).

2.3. Treatment delivery workflow

For daily treatment, patients were positioned in their customized head and neckrest cushion and mask, with a reflective marker placed on their nose to enable HDMM tracking. The HDMM parameter was set at 1.5 mm as a threshold to pause treatment delivery for all patients. A 2.5 mGy localization CBCT was acquired and compared to the reference CBCT scan to assess patient positioning differences and couch adjustments required prior to SRS delivery. CBCTs were automatically registered through the bony anatomy.

For any treatment interruptions, either as required by the patient or triggered through the HDMM threshold, a repeat localization CBCT was required to continue with treatment. The repeat localization CBCT was also registered to the reference CBCT to assess patient positioning differences and required couch adjustments. A post-treatment CBCT was acquired at the end of SRS delivery as tolerated by the patient (i.e. patient did not have to use the washroom, felt discomfort). The number of CBCTs acquired, number and cause of treatment interruptions was prospectively recorded.

2.4. Data collection and analysis

CBCT intra-fraction motion for the treatment fraction was quantified through subtraction of discrepancies between the post-treatment and localization CBCT, registered to the bony skull. Intra-fraction motion was also measured through subtraction of discrepancies between localization and repeat localization CBCTs where patient remasking and repositioning was not required following a treatment interruption. The time stamps for the acquisition of the CBCT (localization, repeat location, post treatment) were identified. The magnitude of the optical data reported during the beginning and end of the CBCT scan was used as the corresponding HDMM measurement. For both CBCT and HDMM data, a three-dimensional vector magnitude was calculated from the intra-fraction displacements in the left–right (L-R), cranial-caudal (C—C), and anterior-posterior (A-P) directions.

Data from the treatment planning database and HDMM tracking logs were post-processed using custom software (MATLAB R2019b, MathWorks Inc., Natick, MA) to determine the vector displacement of the nose marker shift between either the localization CBCT – post-treatment CBCT pair, or the localization – repeat localization CBCT set. As a secondary objective, treatment target location (cerebellum, frontal, occipital, parietal, temporal, multiple targets, and other) and planned treatment time were correlated to HDMM and CBCT intra-fraction motion through the Pearson coefficient (r).

3. Results

The average treatment time for 218 single fraction plans was 62 min (range 12–383 mins), and for 84 multi-fraction plans, 41 min (range 14–103 mins).

A total of 216 pairs of localization - repeat localization, and 260 localization – post-treatment CBCTs were analyzed against HDMM logs. A larger vector magnitude of motion per fraction was consistently observed on HDMM tracking when compared to CBCT measurements (Fig. 1a, b). For the localization – repeat localization pairs, the mean HDMM magnitude as detected by the nose was 1.9 ± 1.0 mm and mean CBCT intra-fraction magnitude measured through the skull was 0.8 ± 0.7 mm (r = 0.06). For the localization – post-treatment pairs, the mean HDMM magnitude was 0.8 ± 1.0 mm and mean CBCT intra-fraction magnitude, 0.7 ± 0.7 mm (r = 0.40). A comparison of repeat localization pairs and localization – post CBCTs is shown in Fig. 1c, where a linear model was created to relate the HDMM to CBCT magnitudes. The model was selected to find a HDMM value for which at least 96 % of the CBCT magnitude values will be less than some ratio of that HDMM value plus a constant, allowing for an accurate selection of a HDMM trigger value. For example, if a HDMM magnitude of 1 mm was measured we could predict that for 96 % of the patients this would result in a CBCT magnitude measurement less than or equal to 1.5 mm.

Figure S1 shows the relationship between HDMM and CBCT measurements triaged by target location. Treatment target location did not improve the correlation between HDMM and CBCT magnitudes (Table 1). The frontal lobe had the highest number of fractions (n = 153), reporting a median (range) of 1.1 (0.1–6.2)mm for HDMM and 0.6 (0.1–2.6)mm for CBCT (r = 0.30). For multiple targets, 111 fractions were assessed, with a median (range) of 1.2 (0–4.4)mm and 0.6 (0.1–2.4) mm for CBCT (r = 30). The highest correlation (r = 0.63) was observed in the other cohort (i.e. pons, falx, parafalcine), but was limited by its small number of fractions analyzed (n = 11).

The number of treatment interruptions for each patient per fraction was recorded. From 489 fractions, 256 (52 %) had no treatment interruptions. There were 120 fractions with 1 interruption, 54 fractions with 2 interruptions, 23 fractions with 3 interruptions, 16 fractions with 4 interruptions, and 20 fractions with 5 or more treatment interruptions. Figure S2a shows a general lack of relationship between target location and number of interruptions, though patients with treatment to multiple targets had the largest number of interruptions, likely due to increased planned treatment time. Figure S2b shows the relationship of increasing interruptions with planned treatment time.

4. Discussion

Intracranial SRS is predicated on accurate treatment delivery to the target while minimizing dose to surrounding organs at risk; frameless immobilization facilitates SRS over multiple sessions and the ability to safely treat larger targets. This study measured intra-fraction motion, characterized between the localization and post treatment time points and within a session resulting in treatment interruptions during SRS, on a large cohort of frameless SRS patients using the HDMM and CBCT system. We found the magnitude of intra-fraction motion detected by the HDMM system were larger than the corresponding CBCT results." with "In this analysis, the intra-fraction motion measured on CBCTs were smaller than those detected by the HDMM system.

In this analysis, we reported intra-fraction motion as a vector magnitude of 0.7 ± 0.6 mm based on CBCT registration. Seneviratne et al reported intra-fraction motion of 0.65 ± 0.46 mm based on CBCT measurements for frameless GK-SRS [12], and Carminucci et al reported slightly higher intra-fraction motion (1.67 ± 2.12 mm) in the superior-inferior axis on a smaller patient cohort [9]. The intra-fraction motion noted by the HDMM system was 1.4 ± 0.9 mm, larger than the corresponding CBCT results. One of the limitations of the study is that the HDMM system logs do not report values less than 0.2 mm, contributing to an overestimation in the HDMM motion error distribution. From our results, a HDMM threshold of 1.5 mm supports the continued use of a 1 mm PTV margin.

In this study, the HDMM to CBCT measurements had a lower correlation for the interruptions in-session (localization – repeat location without remasking). This may be due to patient dependent factors, such as sudden movements caused by sneezing, deep snoring, or waking up

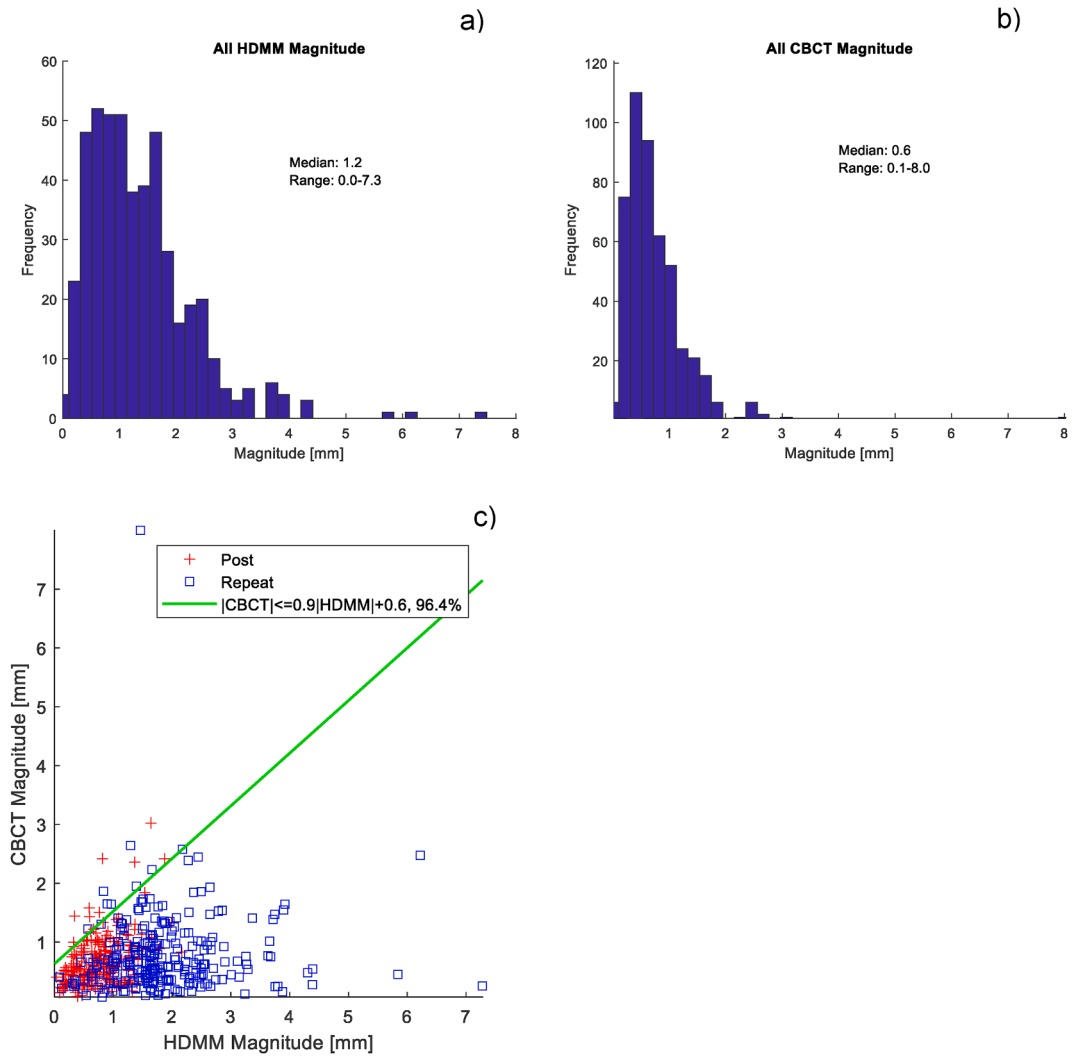

Fig. 1. A) the intra-fraction vector magnitude detected by the hdmm system, and b) the intra-fraction vector magnitude measured on cbcts. c) a scatterplot of cbct magnitude vs hdmm magnitude is shown, triaged between post (localization – post-treatment) and repeat (localization – repeat localization) pairs. a linear model was created to relate the hdmm magnitude to cbct magnitudes. the model was selected to find a hdmm value for which at least 96% of the cbct magnitude values will be less than some ratio of that hdmm value plus a constant, allowing for an accurate selection of a hdmm trigger value.

Table 1
Comparison of median (range) high definition motion management (HDMM) and conebeam CT (CBCT) intra-fraction motion vector magnitudes triaged by target location.

Target Location	N	Median HDMM Magnitude (mm)	Minimum HDMM Magnitude (mm)	Maximum HDMM Magnitude (mm)	Median CBCT Magnitude (mm)	Minimum CBCT Magnitude (mm)	Maximum CBCT Magnitude (mm)	Correlation Coefficient (r)
Cerebellum	61	1.0	0.1	5.8	0.7	0.1	8.0	0.08
Multiple	111	1.2	0.0	4.4	0.6	0.1	2.4	0.30
Frontal	153	1.1	0.1	6.2	0.6	0.1	2.6	0.30
Occipital	46	1.4	0.2	3.8	0.6	0.1	2.4	−0.05
Parietal	48	0.9	0.2	3.7	0.7	0.2	2.4	0.16
Temporal	46	1.4	0.2	7.3	0.6	0.1	1.5	0.00
Other	11	1.1	0.3	2.7	1.0	0.5	1.9	0.63

from sleep. As these large movements occur, the HDMM system tracks and initiates the treatment interruption from inside the treatment bore. As the patient travels out of the machine they may relax back into position, accounting for some of the discrepancies noted between HDMM and CBCT. Patient relaxing as they travel out of the treatment bore, in addition to the increased sensitivity of the HDMM system, may account for the variations noted between the localization to post treatment CBCTs, as the HDMM system consistently reports larger intra-fraction motion.

Our finding of increasing interruptions with treatment time is in agreement with the literature [9–12]. With frameless SRS, it is possible to split treatment for multiple targets over a few days to reduce time on the bed over a single session. MacDonald et al reported modeling with a 5 min test run could predict for treatment interruptions [11]. Since the introduction of frameless GK-SRS at our institution, a trial setup procedure was followed during mask making to ensure patient eligibility.

During trial setup, passive tracking of the marker was performed for 10–20 min while the mask completely hardened to assess the magnitude of patient motion and patient tolerability for treatment. Through this method, we identified patient specific factors, such as those with extreme claustrophobia and poor performance status that precluded them as suitable candidates for frameless SRS (i.e. their inability to stay still would continuously interrupt the HDMM system). These patients were subsequently triaged to the linear accelerator where treatments are shorter and the mask area around their eyes can removed to reduce claustrophobia. From our experience, it is unclear if patient performance during trial setup correlate to the magnitude of intra-fraction motion and number of treatment interruptions.

Frameless SRS is gaining in popularity and utilization due to its improved workflow and ability to provide hypofractionated treatments [13–15], reporting excellent local control when compared to frame patients [16,17]. Various patient satisfaction studies have found from the patient's perspective, the frame is more painful and the mask treatment experience is preferred [18,19]. Our results on this large cohort of patients further supports the use of frameless SRS in the clinical setting.

The analysis in this study was triaged based on target location only, and did not account for target size or the relative distance between the target and nose tip. Our previous study found intra-fraction motion measured through nose tip tracking was consistently greater than CBCT-based movement [5]. Future work will assess the effect of these factors to assess if an improvement in HDMM to CBCT correlation can be found.

There are some limitations when interpreting the results of this study. As the HDMM system reports a vector position based on translational displacements, the effects of rotations measured on CBCTs was not compared. Secondly, though a relatively large sample of patients and treatment fractions were included in this study, the sample size for some of the anatomic locations were small in this preliminary analysis. Finally, for the patients with multiple targets, we did not verify the target at which large intra-fraction motion triggered the HDMM system.

In conclusion, the magnitude of intra-fraction motion detected by the HDMM system were larger than the corresponding CBCT results.

Declaration of Competing Interest

The authors declare the following financial interests/personal relationships which may be considered as potential competing interests: This work was partially supported through a research grant from Elekta and the Canadian Institutes of Health Research (CIHR); the principal investigators of the grants were Dr. David Jaffray and Dr. Caroline Chung.

Appendix A. Supplementary data

Supplementary data to this article can be found online at https://doi.org/10.1016/j.phro.2023.100415.

References

[1] Aoyama H, Shirato H, Onimaru R, Kagei K, Ikeda J, Ishii N, et al. Hypofractionated stereotactic radiotherapy alone without whole-brain irradiation for patients with solitary and oligo brain metastasis using noninvasive fixation of the skull. Int J Radiat Oncol Biol Phys 2003;56(3):793–800. https://doi.org/10.1016/s0360-3016(03)00014-2.

[2] Chang EL, Wefel JS, Hess KR, Allen PK, Lang FF, Kornguth DG, et al. Neurocognition in patients with brain metastases treated with radiosurgery or radiosurgery plus whole-brain irradiation: a randomised controlled trial. Lancet Oncol 2009;10(11):1037–44. https://doi.org/10.1016/S1470-2045(09)70263-3.

[3] Leksell L. The stereotaxic method and radiosurgery of the brain. Acta Chir Scand 1951;102(4):316–9.

[4] Ruschin M, Komljenovic PT, Ansell S, Menard C, Bootsma G, Cho YB, et al. Cone beam computed tomography image guidance system for a dedicated intracranial radiosurgery treatment unit. Int J Radiat Oncol Biol Phys 2013;85(1):243–50. https://doi.org/10.1016/j.ijrobp.2012.03.022.

[5] Li W, Bootsma G, Von Shultz O, Carlsson P, Laperriere N, Millar B, et al. Preliminary Evaluation of a Novel Thermoplastic Mask System with Intra-fraction Motion Monitoring for Future Use with Image-Guided Gamma Knife. Cureus 2016;8(3):e531.

[6] Li W, Cho YB, Ansell S, Laperriere N, Menard C, Millar BA, et al. The Use of Cone Beam Computed Tomography for Image Guided Gamma Knife Stereotactic Radiosurgery: Initial Clinical Evaluation. Int J Radiat Oncol Biol Phys 2016;96(1):214–20. https://doi.org/10.1016/j.ijrobp.2016.04.011.

[7] Wright G, Harrold N, Hatfield P, Bownes P. Validity of the use of nose tip motion as a surrogate for intracranial motion in mask-fixated frameless Gamma Knife((R)) Icon therapy. J Radiosurg SBRT 2017;4(4):289–301.

[8] Wright G, Schasfoort J, Harrold N, Hatfield P, Bownes P. Intra-fraction motion gating during frameless Gamma Knife((R)) Icon therapy: The relationship between cone beam CT assessed intracranial anatomy displacement and infrared-tracked nose marker displacement. J Radiosurg SBRT 2019;6(1):67–76.

[9] Carminucci A, Nie K, Weiner J, Hargreaves E, Danish SF. Assessment of motion error for frame-based and noninvasive mask-based fixation using the Leksell Gamma Knife Icon radiosurgery system. J Neurosurg 2018;129(Suppl1):133–9. https://doi.org/10.3171/2018.7.GKS181516.

[10] Wegner RE, Xu L, Horne Z, Yu A, Goss M, Liang Y, et al. Predictors of Treatment Interruption During Frameless Gamma Knife Icon Stereotactic Radiosurgery. Adv Radiat Oncol 2020;5(6):1152–7. https://doi.org/10.1016/j.adro.2020.06.025.

[11] MacDonald RL, Lee Y, Schasfoort J, Soliman H, Sahgal A, Ruschin M. Real-Time Infrared Motion Tracking Analysis for Patients Treated With Gated Frameless Image Guided Stereotactic Radiosurgery. Int J Radiat Oncol Biol Phys 2020;106(2):413–21. https://doi.org/10.1016/j.ijrobp.2019.10.030.

[12] Seneviratne DS, Vallow LA, Hadley A, Malouff TD, Stross WC, Herchko S, et al. Intracranial motion during frameless Gamma-Knife stereotactic radiosurgery. J Radiosurg SBRT 2020;6(4):277–85.

[13] Vulpe H, Save AV, Xu Y, Elliston CD, Garrett MD, Wu CC, et al. Frameless Stereotactic Radiosurgery on the Gamma Knife Icon: Early Experience From 100 Patients. Neurosurgery 2020;86(4):509–16. https://doi.org/10.1093/neuros/nyz227.

[14] Masucci GL. Hypofractionated Radiation Therapy for Large Brain Metastases. Front. Oncol 2018:8. https://doi.org/10.3389/fonc.2018.00379.

[15] Mengue L, Bertaut A, Ngo Mbus L, Doré M, Ayadi M, Clément-Colmou K, et al. Brain metastases treated with hypofractionated stereotactic radiotherapy: 8 years experience after Cyberknife installation. Radiat Oncol 2020;15(1):82. https://doi.org/10.1186/s13014-020-01517-3.

[16] Wegner RE, Horne ZD, Liang Y, Goss M, Yu A, Pace J, et al. Single Fraction Frameless Stereotactic Radiosurgery on the Gamma Knife Icon for Patients With Brain Metastases: Time to Abandon the Frame? Adv Radiat Oncol 2021;6(5):100736. https://doi.org/10.1016/j.adro.2021.100736.

[17] Grimm MA, Köppen U, Stieler F, Welzel G, Ruder AM, Polednik M, et al. Prospective assessment of mask versus frame fixation during Gamma Knife treatment for brain metastases. Radiother Oncol 2020;147:195–9. https://doi.org/10.1016/j.radonc.2020.05.011.

[18] Li W, Cashell A, Lee I, Tamerou M, Coolens C, Bernstein M, et al. Patient perspectives on frame versus mask immobilization for gamma knife stereotactic radiosurgery. J Med Imaging Radiat Sci 2020;51(4):567–73. https://doi.org/10.1016/j.jmir.2020.08.001.

[19] Pavlica M, Dawley T, Goenka A, Schulder M. Frame-Based and Mask-Based Stereotactic Radiosurgery: The Patient Experience. Compared Stereotact Funct Neurosurg 2021;99(3):241–9. https://doi.org/10.1159/000511587.